

Crystalline Protein Domains and Lipid Bilayer Vesicle Shape Transformations

Margaret R. Horton,^{*,†} Suliana Manley,[†] Silvana R. Arevalo,[†] Alexander E. Lobkovsky,[‡] and Alice P. Gast^{†,§}

Department of Chemical Engineering, Massachusetts Institute of Technology, Cambridge, Massachusetts 02139, Department of Earth, Atmospheric, and Planetary Sciences, Massachusetts Institute of Technology, Cambridge, Massachusetts 02139, and Department of Chemical Engineering, Lehigh University, Bethlehem, Pennsylvania 18015

Received: September 18, 2006; In Final Form: November 1, 2006

Cellular membranes can take on a variety of shapes to assist biological processes including endocytosis. Membrane-associated protein domains provide a possible mechanism for determining membrane curvature. We study the effect of tethered streptavidin protein crystals on the curvature of giant unilamellar vesicles (GUVs) using confocal, fluorescence, and differential interference contrast microscopy. Above a critical protein concentration, streptavidin domains align and percolate as they form, deforming GUVs into prolate spheroidal shapes in a size-dependent fashion. We propose a mechanism for this shape transformation based on domain growth and jamming. Osmotic deflation of streptavidin-coated GUVs reveals that the relatively rigid streptavidin protein domains resist membrane bending. Moreover, in contrast to highly curved protein domains that facilitate membrane budding, the relatively flat streptavidin domains prevent membrane budding under high osmotic stress. Thus, crystalline streptavidin domains are shown to have a stabilizing effect on lipid membranes. Our study gives insight into the mechanism for protein-mediated stabilization of cellular membranes.

Introduction

The lipid bilayer is the base structure for all cell membranes and is a highly flexible material capable of deforming into diverse shapes. In cells, the lipid bilayer membrane is highly heterogeneous and known to contain numerous ordered protein and lipid domains. Proteins are often required to guide and direct the deformation of cell membranes and induce structural transformations important for biological processes including endocytosis.^{1,2} One such protein is clathrin, which assembles on the cellular membrane surface into a well-defined lattice to form invaginations termed clathrin-coated pits that eventually produce internal buds that are part of the endocytotic pathway.^{3–5} This physical process is driven by the fact that the curvature of the clathrin protein lattice exceeds that of the membrane and is believed to influence the size of the clathrin-coated vesicles that are formed.^{4,5} In addition to their role in biological processes, protein arrays on lipid bilayers also have potential application in biosensing and drug delivery, where a well-defined template of proteins can be immobilized on vesicles.⁶

Model systems of proteins on lipid bilayer membranes allow for systematic study of how protein arrays self-assemble and influence lipid membrane shape and curvature. Bacterial surface proteins reconstituted on lipid bilayer vesicles form rigid two-dimensional crystals that deform the membrane into conical and cylindrical shapes.⁷ The tetrameric protein streptavidin also forms two-dimensional crystalline domains when bound to the surface of biotin-functionalized giant unilamellar vesicles (GUVs).^{8,9} Streptavidin-coated GUVs can deform into football-

like prolate shapes when the streptavidin protein domains are aligned and form a continuous envelope.⁸ Micropipet aspiration of streptavidin-coated GUVs shows that the protein-coated bilayer plastically deforms and GUVs crumple as they deflate.⁹ However, the physical mechanisms for how the streptavidin domains align and determine membrane shape have not been systematically explored.

In this study, we investigate the relationship between the configuration of crystalline streptavidin domains and vesicle morphology. The streptavidin-coated membrane system contrasts clathrin-coated membranes because rather than inducing curvature, we find that streptavidin domains flatten membranes and resist membrane bending. We develop a simple model based on domain growth and jamming to account for the shape transformations of the GUVs. We osmotically stress streptavidin-coated GUVs to study how protein-coated bilayers respond to deflation and to qualitatively examine how rigid protein domains influence GUV morphology and stability.

Materials and Methods

Formation of GUVs. GUVs are prepared by the electroformation method¹⁰ from a mixture of 1-stearoyl-2-oleoyl-*sn*-glycero-3-phosphocholine (SOPC, Avanti Polar Lipids, Alabaster, AL) and *N*-((6-(biotinoyl)amino)hexanoyl)-1,2-dihexadecanoyl-*sn*-glycero-3-phosphoethanolamine, triethylammonium salt (biotin-X-DPPE, Invitrogen, Eugene, OR). Lipid mixtures are 10:1 lipid weight ratio (SOPC/biotin-X-DPPE) by mass dissolved in chloroform (HPLC grade, Mallinckrodt, Paris, KY).^{8,9} We add 0.1 mol % of Texas Red 1,2-dihexadecanoyl-*sn*-glycero-3-phosphoethanolamine, triethylammonium salt (TR-DPPE, Invitrogen), to the lipid mixture to label lipid bilayers for confocal fluorescence microscopy experiments. GUVs are formed in 608 mOsm glucose solution and suspended in sucrose to provide optical and density contrast.¹¹ To osmotically stress

* To whom correspondence should be addressed. Telephone: 617-253-6557. Fax: 617-324-6117. E-mail: mhorton@mit.edu.

[†] Department of Chemical Engineering, Massachusetts Institute of Technology.

[‡] Department of Earth, Atmospheric, and Planetary Sciences, Massachusetts Institute of Technology.

[§] Lehigh University.

the GUVs, we suspend glucose-filled GUVs in hyperosmotic sucrose solutions. To achieve higher osmotic stress gradients, we also form vesicles in 300 mOsm glucose.

Coating GUVs with Protein. Electroformed GUVs are incubated in 20 $\mu\text{g}/\text{mL}$ protein solution for at least 3 h to allow crystals to grow and equilibrate on the bilayer surface. Protein solutions are prepared containing streptavidin (Invitrogen), egg white avidin (Sigma-Aldrich), and Alexa Fluor 488-conjugated avidin (Alexa488-avidin, Invitrogen) dissolved in glucose solutions of the same osmolality as those we use to form GUVs. The pH of the GUV and protein solution is adjusted from pH 5.3 to pH 6 using a 500 mM Tris base solution. GUVs are imaged within 12 h of synthesis, but remain stable up to 48 h.

Microscopy. Differential interference contrast (DIC) and fluorescence microscopy images are obtained using a Cooke SensiCam digital camera (Cooke Corporation, Romulus, MI) and a Zeiss Axioplan epifluorescence microscope with 40 \times and 100 \times objectives. Glucose-filled vesicles are diluted 5-fold with 660 mOsm sucrose and placed in CoverWell Perfusion Chambers from Grace Bio-Labs (Bend, OR) sealed to glass slides. To prevent avidin and streptavidin from adhering to the surfaces, the viewing chambers and glass slides are treated by soaking in 1 mg/mL bovine serum albumin solution for 1 h. To measure size distributions of the GUVs, we analyze DIC micrographs using ImageJ software (NIH, Bethesda, MD). GUVs are classified as either spherical or spheroidal; spheroidal GUVs have an aspect ratio greater than 1.1. We determine the minimum curvature of the spheroidal GUVs by fitting a circle to the major vesicle curvature.

For confocal microscopy, we use a Carl Zeiss LSM510 laser scanning confocal microscope at the W.M. Keck Microscopy Facility at the Whitehead Institute. The Zeiss software LSM510 is used to project three-dimensional images measured with 488 and 543 nm excitation lasers and 505/537 and 558/623 bandpass filter sets and either a 40 \times or 100 \times objective (Carl Zeiss). For this inverted microscope apparatus, GUVs are formed in a sucrose solution and re-suspended in a glucose solution.

Osmotic Deflation. To study the retention of solutes within the membrane, GUVs are formed in a glucose solution containing 100 $\mu\text{g}/\text{mL}$ of fluorescein sodium salt (Invitrogen). The GUV solution is diluted in hyperosmotic sucrose to osmotically stress the GUVs. Monitoring the concentrated dye inside the GUVs indicates whether the GUVs leak or rupture.

Results and Discussion

Shape Transformation. When streptavidin binds to a GUV containing biotinylated lipid, it interacts with neighboring streptavidin proteins to form two-dimensional crystalline protein arrays on the surface of the GUV.⁸ When the streptavidin crystals are aligned, GUVs exhibit spheroidal morphology (Figure 1). We visualize the streptavidin crystal morphologies on the surface of fluorescently labeled GUVs by incubating them in a 10:1 weight ratio of streptavidin and Alexa488-Avidin. Avidin binds biotin with an affinity near that of streptavidin but does not crystallize. The fluorescent avidin provides a bright background to visualize streptavidin domains on the GUV surface approximately 5 μm in length. When streptavidin domains are randomly oriented (Figure 1, left), GUVs have spherical morphology. When streptavidin domains align approximately parallel and span the length of the GUV (Figure 1, right), GUVs have football-like shapes which we approximate as prolate spheroid.

Viewing the protein-coated membrane as a composite material, we can qualitatively understand how protein domain

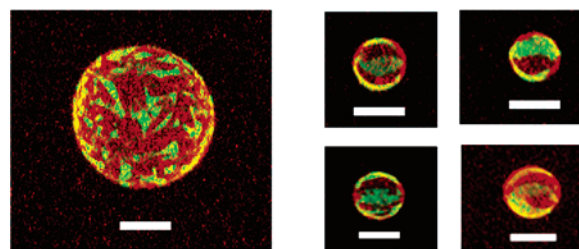


Figure 1. Confocal fluorescence micrographs of protein-coated GUVs synthesized from a lipid mixture containing 0.1 mol % TR-DPPE incubated in solution with 90 wt % streptavidin and 10 wt % noncrystallizable Alexa488-avidin. Bright fluorescently labeled avidin (green) is used to visualize crystalline streptavidin domains on (red) fluorescently labeled bilayer. (Left): Crystals have random orientations and the GUV has spherical morphology. (Right): Large streptavidin crystalline domains align approximately parallel to each other and to the major axis of spheroidal-shaped GUVs. Scale bars are 10 μm .

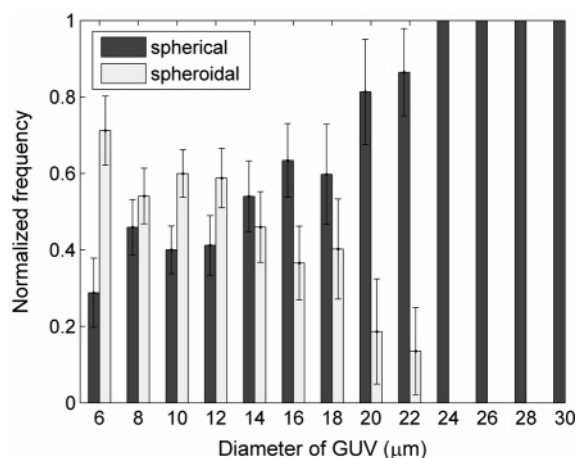


Figure 2. Normalized size distributions of spherical and spheroidal GUVs. Spheroidal GUVs tend to be smaller in size than the spherical GUVs. The GUV diameter of the spheroidal GUVs is defined as the length of the major axis. Error estimated from binomial distribution statistics from $N = 250$ GUV micrographs analyzed.

alignment influences GUV curvature. If the crystalline domains are a rigid, continuous material, then bending along the major axis of the spheroidal GUVs is similar to bending parallel beams. This physical model is supported by the observation that curvatures along the major axes of the spheroidal GUVs in Figure 1, where streptavidin protein domains are aligned, are lower than the curvatures of spherical GUVs. Along the minor axis of the spheroidal GUVs, however, there is not continuous rigid crystalline material, but rather defects between crystalline domains where we expect the membrane to bend more easily. The preference of streptavidin crystals to grow in a planar fashion is consistent with the previous observation of large streptavidin crystals that readily grow up to 100 μm in size on flat bilayer and monolayer surfaces.¹²

Size Trend. An additional observation from Figure 1 is that the spherical GUV (left) is larger in size than the spheroidal GUVs (right). We verify and quantify this trend through analysis of the size and geometry of a population of 250 GUVs coated only with streptavidin and imaged with DIC microscopy. Spheroidal GUVs are defined by having an aspect ratio greater than 1.1. We plot the percent of spheroidal and spherical GUVs at each diameter in Figure 2 to show that smaller GUVs tend to have spheroidal morphology while larger GUVs tend to have spherical morphology. We define the diameter of the spheroidal GUVs as the length of the major axis. Although spheroidal GUVs are observed with a range of sizes, their proportions

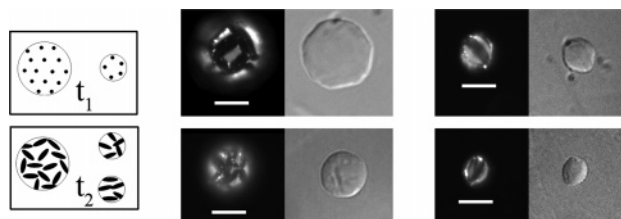


Figure 3. Model for crystalline domain growth and size trend. (Left): Illustration of crystal domain growth at two different time scales. At time t_1 , the number of nucleation sites per unit area is constant for all membrane surfaces, and at a later time t_2 , domains have a greater probability of aligning on smaller GUVs. (Middle and right): Fluorescence and DIC micrographs of GUVs incubated in 90 wt % streptavidin and 10 wt % Alexa488-avidin protein solution. Spherical GUVs (middle) are larger than spheroidal GUVs (right). Spherical GUVs have more crystal domains that are randomly oriented than spheroidal GUVs, which have aligned domains. All scale bars are 10 μm .

remain approximately constant with aspect ratio defined as the length of the major axis over the length of the minor axis of 1.18 ± 0.08 . This suggests that the curvature of the surface on which the streptavidin crystals grow influences the preferred curvature of the crystals that are formed. Smaller GUVs have higher curvature than larger GUVs; thus, streptavidin crystals growing on smaller GUVs must conform to a higher membrane curvature than crystals grown on larger GUVs or planar bilayers.

We propose a crystal growth and jamming model to account for the observation that spheroidal GUVs tend to be smaller. We assume that the number of nucleation sites per unit area is constant for all lipid bilayer surfaces, as illustrated by the schematic in Figure 3 (left), showing the early nucleation of protein domains on both a large and a small GUV at time t_1 . At a later time, t_2 , the protein domains have grown and begin to contact adjacent domains. We define jamming as the state at which protein domains are in contact with one another and are no longer able to grow. For simplicity, we assume that, for a given GUV, the growth rate of the domains is the same on all surfaces of that GUV. If the protein domains have random orientations as they begin to grow, then the probability of having aligned domains is increased on the smaller GUVs because there are fewer protein domains. In other words, the fractional probability of N objects with random orientations on a grid of size N having the same orientation scales exponentially as $\sim N$; therefore, smaller grids, or smaller GUVs with fewer protein domains, have a higher probability of alignment. The basis for these assumptions is confirmed by fluorescence and DIC micrographs in Figure 3, which demonstrate that larger GUVs have more domains than smaller GUVs and that the length of the streptavidin domains does not depend on the size of the GUV on which they grow.

To verify the consistency of this physical picture, we estimate the time scales for the protein domains to grow and diffuse. Streptavidin crystals have a preferred growth direction on biotinylated GUVs, with C222 crystal lattice structure.¹² The rate of streptavidin domain growth along the preferred growth direction measured on monolayers is 1–50 $\mu\text{m}/\text{min}$.¹³ We take the lower value of 1 $\mu\text{m}/\text{min}$ because our low ionic strength solution conditions should slow protein crystalline growth.¹² Based on this growth rate, crystals reach their 5 μm length within 5 min. We compare this time scale to the approximate time scale for the protein domains to rotate in the membrane. The rotational diffusion, D_R , of a molecule of length rotating in a membrane with viscosity μ can be calculated from the equation

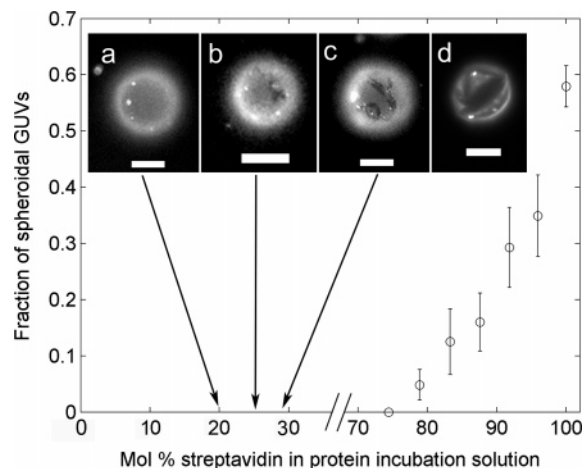


Figure 4. Streptavidin domain morphology and GUV shape transformation depend on concentration of streptavidin. Graph of the measured relationship between the fraction of GUVs observed having a spheroidal morphology and the amount of streptavidin in the streptavidin/avidin protein incubation solution used to coat GUVs. Error is estimated from binomial distribution statistics of $N = 411$ micrographs analyzed. Fluorescence micrographs of GUVs incubated in protein solution with varied concentrations of streptavidin. Mol % of streptavidin in incubation solution is (a) 20 mol %, (b) 25 mol %, (c) 29 mol %, and (d) 90 mol %. The remaining protein incubation solution contains 10 mol % Alexa488-avidin and the balance egg white avidin. (a): No microscopic protein domains are observed on GUVs incubated in 20 mol % streptavidin solution. All scale bars are 10 μm .

$$D_R = \frac{k_B T}{8\pi\mu l^3} \quad (1)$$

where k_B is Boltzmann's constant and T is temperature. We calculate the membrane viscosity, $\mu = 9 \times 10^{-2}$ Pa·s, using the Stokes–Einstein equation and the estimated diffusivity of monomolecular streptavidin,¹³ $D_T = 5 \times 10^{-9}$ cm^2/s . We can use this to calculate the rotational diffusion coefficient D_R and the characteristic time scale for domain rotation,¹⁴ $t_R \sim 1/D_R$, over a range of streptavidin domain sizes. We find that $t_R \sim 0.5$ s when domains are 0.1 μm in size and we estimate $t_R \sim 70$ min when domains are 2 μm in size. Comparison of the rotational diffusion time scales with our estimated time scale for crystal growth indicates that the domains grow much faster than they rotate. As the domains grow quickly on the GUV surface, they are not free to rotate and they approach a jammed configuration.

Effect of Streptavidin/Avidin Ratio on Shape Transformation. An important consideration in understanding how the arrangement of jammed streptavidin domains on the GUV surface influences vesicle shape is the surface coverage of crystalline streptavidin. By adjusting the relative amounts of avidin and streptavidin in the protein incubation solution, we can control the surface coverage of crystalline streptavidin relative to noncrystalline avidin. The fraction of GUVs transformed into a spheroidal shape increases as the concentration of streptavidin in the protein solution increases, as shown in Figure 4. The minimum amount of streptavidin in the protein solution required to observe spheroidal GUVs is 74–78 mol % streptavidin. Micrographs (Figure 4b–d) illustrate that the surface coverage of streptavidin crystals increases as the concentration of streptavidin in the GUV incubation solution increases. The approximate amount of streptavidin required to observe microscopic crystals with optical microscopy is 25 mol % streptavidin (Figure 4b). This minimum concentration

threshold is comparable to streptavidin crystallization threshold observed on monolayers¹³ of 15 mol %.

Consideration of the geometry and coverage of protein crystals near the sphere-to-spheroid shape transformation threshold allows us to qualitatively describe the mechanism for spheroidal GUV formation. We observe that spheroidal GUVs require an aligned continuous network of crystalline streptavidin domains along their major axes, which requires a minimum coverage of streptavidin. Therefore, we qualitatively describe the onset of the sphere-to-spheroid GUV shape transformation as an aligned percolation process, where microscopic streptavidin domains are the percolating material. Once protein domain coverage enables the formation of a continuous network spanning the GUV length, a percolation threshold is reached and the percolated protein network can deform GUVs into a spheroidal geometry. In our system, we observe spheroidal GUVs beginning at streptavidin concentrations of ~ 75 mol %; fluorescent micrographs suggest that, below this streptavidin concentration, the coverage of protein crystals is insufficient to form a continuous material spanning the membrane dimension (Figure 4b,c). At streptavidin concentrations above the shape transition threshold, we observe an approximately linear dependence of the amount of shape-transformed GUVs on the concentration of streptavidin in the protein incubation solution (Figure 4).

Our observations are qualitatively similar to other studies of two-dimensional percolation of objects with elongated geometry. Studies of randomly oriented sticks and their two-dimensional percolation in an aligned direction as a function of stick concentration and stick alignment show a similar trend, where the probability of percolation increases approximately linearly as the concentration of sticks increases.¹⁵ We estimate the surface coverage of streptavidin crystals at percolation using results for 2-D randomly oriented overlapping ellipses. If we approximate the streptavidin crystalline domains as ellipses with aspect ratio of 2–3, then the approximate coverage of the ellipsoidal domains in a 2D system at percolation, p_c , can be calculated as $1 - p_c$, where p_c is the area fraction of the surface not covered with overlapping ellipses. The formula to estimate p_c as a function of the ellipses' aspect ratio b/a is¹⁶ $p_c = (1 + 4y)/(19 + 4y)$ and $y = b/a + a/b$. We estimate the net area covered by overlapping ellipses, or the streptavidin crystalline domains, at the percolation threshold to be 0.56–0.62. In our system, the approximate fraction of the GUV surface covered by streptavidin domains when GUVs are coated with 90 mol % streptavidin is ~ 0.5 . This measurement is only an approximation, as we are limited by using 2D images to approximate a 3D surface; however, it suggests that the coverage of streptavidin domains when GUVs incubate in a solution containing 90 mol % streptavidin is sufficient to span the surface of the GUVs and thus enable observation of spheroidal GUVs.

Osmotic Stress Response of GUVs. Osmotically stressing our protein-coated vesicles allows us to more thoroughly investigate how the streptavidin domains resist bending and determine the GUV shape and stability. Osmotic deflation of lipid bilayer vesicles can be used to characterize membrane topology¹⁷ and vesicle shape transformations.¹⁸ We osmotically deflate the glucose-filled GUVs by placing them in a concentrated sucrose medium; the resulting hyperosmotic environment causes the vesicles to lose part of their internal water volume to equilibrate the osmolarity of the external and internal solutions.¹⁹ Streptavidin-coated GUVs viewed in a hyperosmotic sugar environment have two distinct morphologies: roughened spherical or spheroidal, with a ridge along the vesicle major

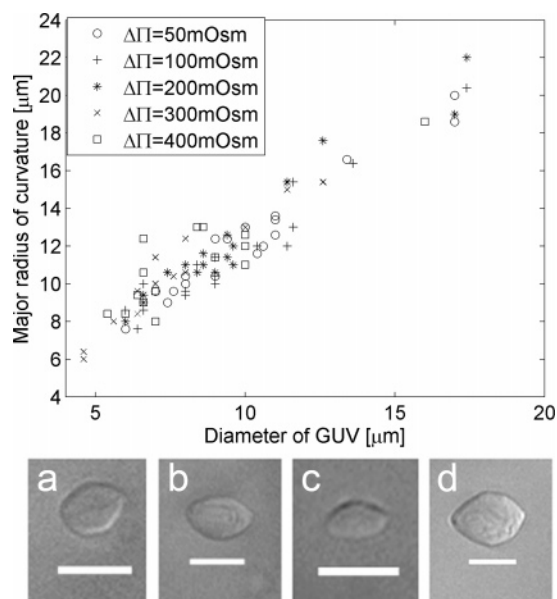


Figure 5. Spheroidal GUVs maintain their shape under osmotic stress. (Above): Measurement of the minimum curvature of spheroidal GUVs at different osmotic stress gradients for $N = 68$ GUVs. The ratio of the minimum curvature to the GUV diameter for the spheroidal GUVs is approximately constant. (Below): DIC micrographs of streptavidin-coated GUVs deflated with osmotic stress gradients of (a) $\Delta\text{Osm} = 100$ mOsm, (b) 200 mOsm, (c) 300 mOsm, and (d) 400 mOsm. All scale bars are 10 μm .

axis.⁸ Interestingly, under increasing osmotic stress spheroidal GUVs maintain their major axes and proportions. Figure 5 shows the measured curvatures of different populations of spheroidal GUVs subjected to osmotic stress gradients $\Delta\text{Osm} = 50$ –400 mOsm (Figure 5). Though we vary the osmotic gradient used to stress the GUVs, the ratio of major curvature to GUV diameter remains approximately constant. DIC micrographs illustrate how the spheroidal GUVs maintain their morphology even under high osmotic stress (Figure 5a–d).

We compare the osmotic stress responses of bare GUVs and GUVs coated with crystalline vs noncrystalline protein to examine how ordered protein domains affect the bending properties of the lipid bilayer. Bare, streptavidin/avidin, and avidin-coated GUVs remain spherical when they are not osmotically stressed (Figure 6, left column). Streptavidin domains, however, slightly deform the membrane even in the absence of osmotic stress (Figure 6b, left column). Upon application of an osmotic stress, bare, uncoated vesicles can produce internal daughter vesicles (Figure 6i) and become flaccid (Figure 6ii). These shape and topological transformations resulting from the decrease in vesicle volume have been observed^{17–21} and characterized in terms of the bending energy and mechanics of lipid bilayers.²² Crystalline protein domains prevent the shape and topological transformations typically observed for lipid bilayers. GUVs coated with streptavidin have a wrinkled morphology upon osmotic stressing and shrink anisotropically (Figure 6b, right column). Osmotically deflated spherical GUVs have a wrinkled appearance with many facets (Figure 6iii). In contrast, spheroidal GUVs maintain their major axes under osmotic stress (Figure 6iv). Comparing crystalline and noncrystalline protein coatings further reveals the impact of the crystalline domains on the osmotic deflation response of the GUVs. When coated with a mixture of avidin and streptavidin, osmotically stressed GUVs have a wrinkled morphology similar to GUVs incubated in only streptavidin (Figure 6c, right column). This contrasts the behavior of the avidin-coated

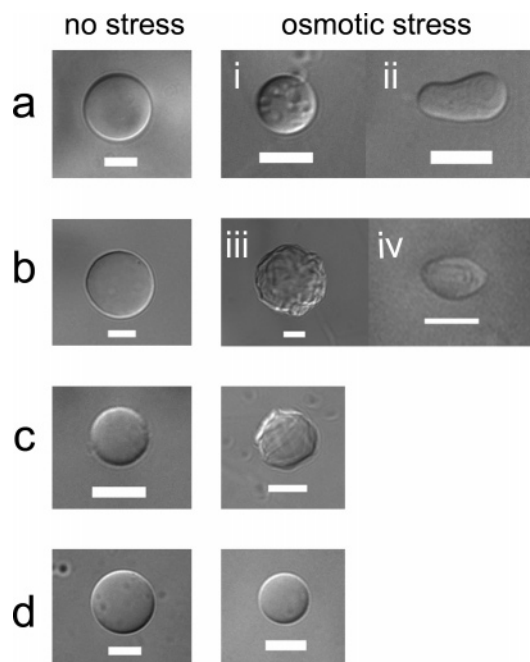


Figure 6. DIC micrographs of GUVs with and without applied osmotic stress. (a): Bare GUVs lacking crystalline protein with no osmotic stress (left column) and with $\Delta\text{Osm} = 250$ mOsm osmotic stress (right column). Osmotically stressed membranes produce daughter vesicles (i) or become flaccid (ii). (b): GUVs incubated in streptavidin protein solution unstressed (left) and osmotically stressed (right) with approximately spherical geometry at $\Delta\text{Osm} = 200$ mOsm osmotic stress (iii) and spheroidal geometry at $\Delta\text{Osm} = 200$ mOsm (iv). (c): GUV incubated in 50 wt % streptavidin/50 wt % avidin protein solution without stress (left) and with $\Delta\text{Osm} = 250$ mOsm (right). (d): GUV incubated in avidin protein solution without stress (left) and with $\Delta\text{Osm} = 250$ mOsm (right). All scale bars are $10\ \mu\text{m}$.

vesicles (Figure 6d), which maintain a smooth, spherical morphology when stressed but resist budding or the formation of daughter vesicles. Avidin-coated vesicles often rupture even in the absence of osmotic stress gradients and few GUVs are present at osmotic gradients above $\Delta\text{Osm} = 250$ mOsm. This effect may be due to the affinity of the avidin-coated GUVs for the glass surfaces that has been previously observed.⁹

We visualize the wrinkles and facets of osmotically stressed streptavidin-coated vesicles in more detail with confocal fluorescence microscopy and fluorescently labeled lipid in Figure 7. Equatorial micrographs of spherical GUVs (Figure 7a–c) illustrate the wrinkled or folded regions of the fluorescently labeled lipid bilayer that form when the protein-coated membrane is deflated by osmotic stress. Folded features become deeper and have higher local curvature as the concentration gradient is increased. Spheroidal GUVs exhibit concentrated lipid folding along their major axes (Figure 7d). The lipid fold in Figure 7d penetrates the GUV to a depth of approximately 33% of the total depth of the spheroidal GUV. This confirms our expectation that the membrane should yield along the defects between streptavidin crystalline domains, which are at a higher density in this minor axis direction.

Osmotic deflation experiments also allow us to investigate how protein coatings on lipid bilayers influence topological membrane transformations such as budding. Our microscopy data suggest that the overall surface area of the protein-coated membrane is conserved despite osmotic deflation and that membrane budding at high osmotic stress is suppressed by the streptavidin crystals. In contrast, proteins with high intrinsic curvature that coat lipid membranes can assist in membrane budding.^{1,2} Clathrin protein assembles in pits that form detaching

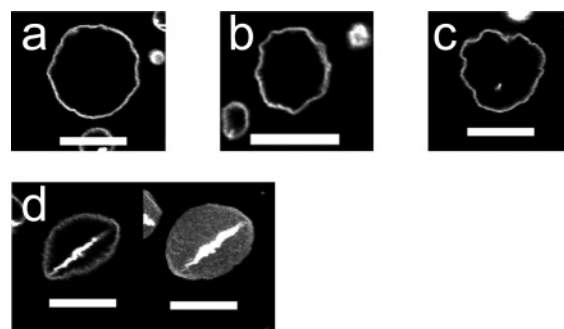


Figure 7. Confocal fluorescence micrographs of GUVs synthesized from lipid mixture containing 0.1 mol % TR-DPPE coated with streptavidin subjected to osmotic stress gradients. (a–c): Equatorial micrographs of GUVs under osmotic stress (a) $\Delta\text{Osm} = 100$ mOsm, (b) 200 mOsm, and (c) 300 mOsm, illustrating the highly curved wrinkles in the vesicle lipid bilayer. (d): Equatorial section (left) and projection image (right) of GUV with $\Delta\text{Osm} = 200$ mOsm. Approximate GUV dimensions are $12\ \mu\text{m}$ in z -depth and $14\ \mu\text{m}$ in length and equatorial image is taken at a depth of $2.5\ \mu\text{m}$ into the GUV; the folded portion of the bilayer extends $4\ \mu\text{m}$ into GUV. All scale bars are $10\ \mu\text{m}$.

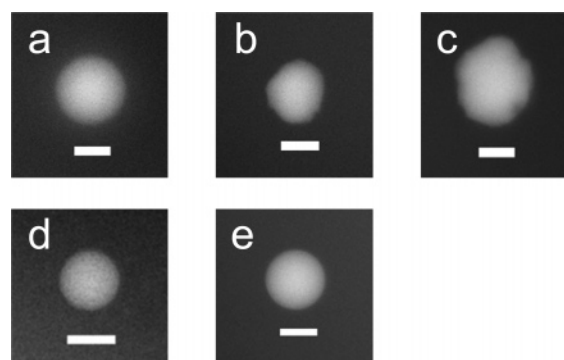


Figure 8. Fluorescence micrographs of GUVs encapsulating fluorescein. (a–c): GUVs incubated in streptavidin protein solution. (d,e): GUVs lacking protein coating. (a,d): No osmotic stress applied. (b,c,e): GUVs osmotically stressed with $\Delta\text{Osm} = 250$ mOsm (b,e) and $\Delta\text{Osm} = 500$ mOsm (c). No bare GUVs are observed at $\Delta\text{Osm} = 500$ mOsm. All scale bars are $10\ \mu\text{m}$.

buds for cell endocytosis. The lattice formed by the clathrin proteins is highly curved and this protein curvature determines the size of the budded internal vesicles that are formed.^{4,5} Our osmotic deflation experiments suggest that tethered protein domains on lipid membranes with intrinsic curvature lower than the membrane curvature can prevent membrane budding and locally increase membrane rigidity. A third category of disordered protein coatings is avidin, which we show prevents budding under moderate osmotic stress of $\Delta\text{Osm} = 250$ mOsm (Figure 6d, right column). The mechanism of how noncrystalline avidin suppresses budding is unclear. The general question of how disordered protein coatings affect lipid curvature is important in cells, however, as diverse protein species reside in the membrane.

Osmotically stressed streptavidin-coated vesicles present a crumpled shape, with small regions of very high membrane curvature that may be expected to affect the integrity of the lipid bilayer. To investigate this, we study the retention of a small molecule chromophore encapsulated in the vesicles. The retention or leakage of an encapsulated dye indicates whether the bilayer is porous, ruptured, or torn. Figure 8 demonstrates how the protein-coated lipid bilayer resists rupture and leakage under osmotic stress. The retention of fluorescein sodium salt (hydrodynamic radius $R_H \sim 0.5$ nm) within the vesicles coated

with protein (Figure 8a–c) indicates that no nanometer-sized holes form in the bilayer even under significant osmotic stress of $\Delta\text{Osm} = 500$ mOsm (Figure 8c). Even after 12 h, the protein-coated GUVs retain the dye with no leakage measured by fluorescence. Bare vesicles (Figure 8d,e) retain the dye and resist rupture upon osmotic stressing of $\Delta\text{Osm} = 250$ mOsm (Figure 8e). Interestingly, at osmotic stress gradients greater than 300 mOsm, no bare GUVs remain in the sample due to membrane collapse and rupture. We verify this effect in experiments with GUVs containing fluorescently labeled lipid subjected to osmotic stress gradients (data not shown). The stability of protein-coated GUVs compared to bare unstable GUVs at $\Delta\text{Osm} = 500$ mOsm indicates that the crystalline protein layer protects the membrane. Crystalline proteins on bilayers in nature may protect primitive organisms. S-layers on the surface of archaea and bacteria are crystalline protein coatings that are linked to the plasma membrane.²³ A possible function attributed to S-layers is protection of the archaea. Our findings are consistent with previous studies suggesting that S-layers stabilize model membranes subjected to mechanical stress.⁶

Conclusions

Understanding the physical mechanism of the assembly and ordering of proteins on the lipid bilayer and their effect on the membrane curvature gives insight into the biophysical processes of membrane bending and cell shape changes. Our system of streptavidin crystallized on GUVs containing biotinylated lipid illustrates how a coating of ordered protein domains can change the physical properties of the membrane. We demonstrate that the configuration of the proteins on the lipid membrane surface determines the shape of the GUVs, as aligned domains resist bending preferentially in one direction. This model biological membrane system provides an interesting experimental platform for studying the physical phenomena of two-dimensional percolation and jamming. We also demonstrate that crystalline protein domains on the GUV surface prevent vesicle budding and protect the lipid bilayer from rupture or leakage upon

osmotic deflation. Our findings suggest that protein arrays on cellular membranes play an important role in cell shape determination and membrane stabilization.

Acknowledgment. We thank Corey O'Hern for useful discussions, Nicki Watson for advice and instruction in confocal microscopy, and Poe Ratanabanangkoon for assistance with experimental protocol. This work was funded through a National Science Foundation Graduate Research Fellowship to M.R.H.

References and Notes

- (1) McMahon, H. T.; Gallop, J. L. *Nature* **2005**, *438*, 590.
- (2) Farsad, K.; De Camilli, P. *Curr. Opin. Cell Biol.* **2003**, *15*, 372.
- (3) Heuser, J. E.; Keen, J. J. *Cell Biol.* **1988**, *107*, 877.
- (4) Mashl, R. J.; Bruinsma, R. F. *Biophys. J.* **1998**, *74*, 2862.
- (5) Nossal, R. *Traffic* **2001**, *2*, 138.
- (6) Mader, C.; Küpcü, S.; Sára, M.; Sleytr, U. B. *Biochim. Biophys. Acta* **1999**, *1418*, 106.
- (7) Paul, A.; Engelhardt, H.; Jakubowski, U.; Baumeister, W. *Biophys. J.* **1992**, *61*, 172.
- (8) Ratanabanangkoon, P.; Gropper, M.; Merkel, R.; Sackmann, E.; Gast, A. P. *Langmuir* **2002**, *18*, 4270.
- (9) Ratanabanangkoon, P.; Gropper, M.; Merkel, R.; Sackmann, E.; Gast, A. P. *Langmuir* **2003**, *19*, 1054.
- (10) Angelova, M. I.; Soleau, S.; Meleard, P.; Faucon, J.-F.; Bothorel, P. *Prog. Colloid Polym. Sci.* **1992**, *89*, 127.
- (11) Döbereiner, H.-G.; Käs, J.; Noppl, D.; Sprenger, I.; Sackmann, E. *Biophys. J.* **1993**, *65*, 1396.
- (12) Ratanabanangkoon, P.; Gast, A. P. *Langmuir* **2003**, *19*, 1794.
- (13) Ku, A. C.; Darst, S. A.; Kornberg, R. D.; Robertson, C. R.; Gast, A. P. *Langmuir* **1992**, *8*, 2357.
- (14) Saffman, P. G.; Delbrück, M. *Proc. Natl. Acad. Sci. U.S.A.* **1975**, *72*, 3111.
- (15) Du, F.; Fischer, J. E.; Winey, K. I. *Phys. Rev. B* **2005**, *72*, 121404.
- (16) Xia, W.; Thorpe, M. F. *Phys. Rev. A* **1988**, *38*, 2650.
- (17) Ménager, C.; Cabuil, V. *J. Phys. Chem. B* **2002**, *106*, 7913.
- (18) Mathivet, L.; Cribier, S.; Devaux, P. F. *Biophys. J.* **1996**, *70*, 1112.
- (19) Viallat, A.; Dalous, J.; Abkarian, M. *Biophys. J.* **2004**, *86*, 2179.
- (20) Guedeau-Boudeville, M.-A.; Bernard, A.-L.; Bradley, J.-C.; Singh, A.; Jullien, L. In *Giant Vesicles*; Luisi, P. L., Walde, P., Eds.; John Wiley & Sons Ltd.: Chichester, U.K., 2000; Chapter 26.
- (21) Hotani, H. *J. Mol. Biol.* **1984**, *178*, 113.
- (22) Seifert, U.; Berndl, K.; Lipowsky, R. *Phys. Rev. A* **1991**, *44*, 1182.
- (23) Sleytr, U. B.; Sára, M.; Pum, D.; Schuster, B. *Prog. Surf. Sci.* **2001**, *68*, 231.